

## Natural Convection Flow and Heat Transfer in Square Enclosure Asymmetrically Heated from Below: A Lattice Boltzmann Comprehensive Study

Taoufik Naffouti<sup>1,2</sup> and Ridha Djebali<sup>1,3</sup>

**Abstract:** This paper reports numerical results of natural convection flow evolving inside confined medium defined by two-dimensional square enclosure containing isothermal hot source placed asymmetrically at bottom wall. The sides-walls are isothermally cooled at a constant temperature; however the ceiling and the rest of bottom wall are insulated. The lattice Boltzmann method is used to solve the dimensionless governing equations with the associated boundary conditions. The flow is monitored by the Grashof number and the Prandtl number taken here 0.71. Numerical simulations are performed to study the effects of Grashof number ranging from  $10^4$  to  $10^6$ , hot source length from 0.1 to 0.4 and its position ranging from 0.15 and 0.45, on flow and heat transfer behaviours. It was found that the developed lattice Boltzmann thermal model give credible results by comparison with former findings. Additionally, it was found that the Grashof number increase as well as the source length results in enhancing the convective currents and then heat transfer rate quantified by the Nusselt number along the hot source. Besides, the variation of the hot source position affects the dynamic and thermal structures and increases slightly the heat transfer to a rate of 5%.

**Keywords:** Natural convection, heat transfer, partially heated square enclosure, numerical simulation, lattice Boltzmann computer modeling.

---

<sup>1</sup> Univ. Tunis El-Manar, LETTM, 2092 Manar 2, Tunis, Tunisia.

<sup>2</sup> Email: taoufik\_naffouti@yahoo.fr

<sup>3</sup> CNRS-SPCTS / CEC 12, Rue Atlantis 87068, Limoges, France.

**Nomenclature**

$\vec{e}_\alpha$	Discrete lattice velocity	$Nu_0$	Nusselt number at the hot wall
$\vec{x}$	Lattice node in $(x,y)$ coordinates	$Gr$	Grashof number $g\beta\Delta TH^3/\nu^2$
$\vec{u}$	Velocity vector $(u, v)$	<b>Greek symbols</b>	
$\vec{g}$	Gravity field	$\omega_\alpha$	Weighting factors
$c_s$	Lattice sound speed	$\rho$	Fluid density (volumetric mass)
$f_\alpha, g_\alpha$	Discrete distribution functions.	$\rho_0$	Reference fluid density
$H$	Height of the enclosure	$\nu$	Kinematic viscosity
$p$	Ideal gas pressure $\rho c_s^2$	$\chi$	Thermal diffusivity
$\theta$	Dimensionless temperature field	$\tau_f, \tau_g$	Relaxation times for $f_\alpha$ and $g_\alpha$
$\Delta T$	Horizontal temperature gradient $T_h - T_c$	$\beta$	Thermal expansion coefficient
$\Delta t$	Time step	<b>Subscripts Suscripts</b>	
$\Delta x$	Lattice spacing units $(=\Delta y)$	$eq$	Equilibrium part
$Pr$	Prandtl number $\nu/\chi$	$\alpha$	Discrete velocity direction

**1 Introduction**

Study of natural convection phenomena is of particular and continuous importance since the broad range of responses made for numerous applications of classical and recent interest. Besides, natural convection in square enclosures plays a very interesting role in several engineering applications, such as solar energy systems, cooling of electronic devices, air conditioning, etc. . . which, therefore, has met with particular interest from industrial and computational fluid dynamic researchers.

In scientific literature a great number of studies deals with natural convection in square enclosures, majority of them treat this topic through numerical simulation. Perusal of prior and recent numerical studies by Djebali and ElGanaoui (2011), Alama, Kumar et al. (2012), Djebali, ElGanaoui, and Naffouti (2012) and Nor-Azwadi and Izual (2012) reveal that several attempts have been made to acquire a basic understanding of natural convection flows and heat transfer characteristics in enclosures.

Besides, investigation of natural convection flow and heat transfer in enclosure heated totally / partially from below is met with significant attention by researchers. To analyse the convective transport in a magma chamber, Chu, and Hichox (1990) carried out an experimental and numerical study of natural convection in an enclosure with localized heating from below. Computer modeling and flow visualization showed that the flow field consists of two counter- rotating cells driven by a central plume rising from the heated wall. Ganzorolli and Milanez (1995) analyzed natural convection in an enclosure heated from below and symmetrically cooled from the sides. The effects of the Rayleigh number, the Prandtl number and aspect ratio on the flow and energy transport were determined. For the square cavity, uniform surface temperature or uniform heat flux does not strongly affect the flow or the

isotherm contours. In the case of uniform temperature at the cavity floor, it has been shown that the cavity is not always thermally active along its whole extension and the flow does not fill it uniformly. Lakhali et al. (1995) investigated numerical natural convection in a square enclosure heated periodically partially from bottom wall. It has been found that heat transfer is the higher when the heating element is positioned at the center of the enclosure. For high Rayleigh number, an increase in the period of the heating element temperature oscillation causes the elimination of the predominance of the positive cell with regard to that of the negative cell during each flow period oscillation. Turgoklu and Yucel (1995) studied the effect of heater and cooler locations on natural convection in square cavities. It was noted that the mean Nusselt number increases as the heater moves closer to the bottom wall.

Ramos and Milanez (1998) carried out an experimental and numerical analysis for natural convection flow caused by heat sources dissipating energy at a constant rate. This source simulates electronic components mounted at the bottom surface of a cavity symmetrically cooled from the sides and insulated at the top. Aydin and Yang (2000) have numerically investigated the natural convection of air in a vertical square cavity with localized isothermal heating from below and symmetrical cooling from sidewalls. The effect of varying the source length symmetrically shows that the flow and temperature fields are vertically symmetric in the enclosure and that for high Rayleigh number the heat transfer is dominated by convection mode. Corcione (2003) has examined numerically a steady laminar natural convection in two-dimensional enclosures heated from below and cooled from top for different thermal boundary conditions at the sidewalls. Author concluded that the heat transfer effectiveness of the bottom wall increases as each adiabatic side-wall is replaced by a cooled side-wall. An opposite behavior is observed for the ceiling. A numerical investigation on natural convection in a glass-melting tank heated locally from below has been performed by Sarris et al. (2004). For small Rayleigh number, the heat transfer is dominated by conduction; while for higher Ra, convection becomes dominant. Increase of the tank aspect ratio and the heated strip width intensifies the fluid flow and increases the thermal field.

Calgagni et al. (2005) investigated experimentally and numerically free convective heat transfer in a square enclosure characterized by a discrete heater located on the bottom wall and cooled from the side walls. The local Nusselt number evaluated at source surface shows a symmetrical profile raising near the heat source boundaries. Massimo et al (2006) studied the influence of a small heating source position on the natural convective heat transfer in a square cavity. It was found that increasing the Rayleigh number enhances the convective currents and heat transfer. The configuration with the heat source placed centrally shows a symmetrical behaviour and therefore a symmetrical distribution of local Nusselt number. Saha et al. (2007)

studied natural convection in enclosure with discrete isothermal heating from below. Authors state that as Grashoff number increases, natural convection dominates and the temperature variation is restricted over a gradually diminishing region around the heat source. Che Sidik (2009) used the Lattice Boltzmann method to exam the isotherms and streamlines of flow in a square cavity with partially heated from below and symmetrical cooled from sides. As the Rayleigh number increases, the intensity of the recirculation inside the cavity increases and the cores of cells move upwards. Paroncini and Corvaro (2009) carried out an experimental and numerical study of natural convection in a square enclosure with a hot source. Author shows that the velocity magnitude and the average Nusselt number increase with the Rayleigh number increase.

Besides, numerical simulation and modeling using LB method becomes a challenging branch in CFD [Guo and Zhao (2005); Chatterjee (2010); Djebali, Pateyron and ElGanaoui (2011)]. For instance, the LBM enjoys second order accuracy in time and space, efficient computational facilities and has met with significant success for numerical simulation and modeling of flows in many areas of classical or current interest and complex problems [Djebali, ElGanaoui and Pateyron (2011); Djebali, Sammouda and ElGanaoui (2011); Lou, Guo and Zheng (2011)].

The previous researchers offer a significant contribution to experimental and numerical studies of natural convection in confined media heated from below. Nevertheless, it is interesting to understand the average thermal and dynamic fields of natural convection in 2D square enclosure with discrete asymmetrical-isothermal heating from below. A D2Q9-D2Q9 double population thermal lattice Boltzmann (LB) model used in the present study to carry out the effects of Grashof number, hot source length and its position on flows and heat transfer behavior in square enclosure.

## 2 Computational aspects

### 2.1 Configuration model

In the present work, a square enclosure of dimensions  $H \times H$  is considered as shown in Fig. 1. A hot source set at constant temperature  $T_h$  is located at the bottom wall and centered at  $x_c$  from the left. The ceiling is thermally insulated and the side-walls are isothermally cooled at a constant temperature  $T_c$ .

In this study, we aim investigating the thermal and dynamic behaviours and heat transfer in such configuration under effects of varying the Grashof number from  $10^4$  to  $10^6$ , the source length  $\varepsilon$  from 0.2 to 0.4 (for a centred heat source) and the source-centre position  $x_c$  from 0.15 to 0.45.

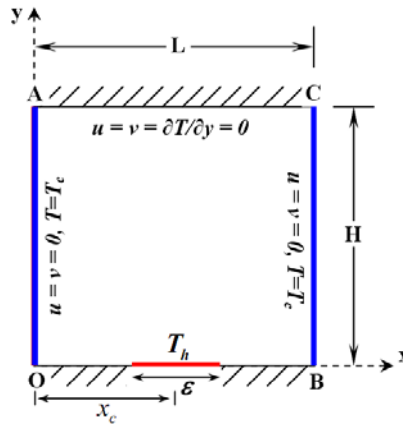


Figure 1: Sketch of the square enclosure partially heated from below.

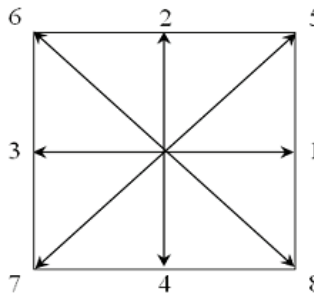


Figure 2: The nine-velocity LB model on 2D square lattice

### 2.2 Background of the thermal lattice Boltzmann model

The lattice Boltzmann approach is considered in this study to simulate natural convection flow and heat transfer in a square medium. In the LB method, the fluid is modelled by fictitious particle exchanging informations quantified by distribution functions that occupy nodes and transit to neighbouring nodes in a streaming phase. The time evolution of the distribution functions in the present double population’s thermal model D2Q9-D2Q9 in the presence of source term is written as follows:

$$f_{\alpha}(\vec{x}', t') - f_{\alpha}(\vec{x}, t) = -\frac{1}{\tau_f} [f_{\alpha}(\vec{x}, t) - f_{\alpha}^{eq}(\vec{x}, t)] + \delta t F_{\alpha} \tag{1}$$

$$g_{\alpha}(\vec{x}', t') - g_{\alpha}(\vec{x}, t) = -\frac{1}{\tau_g} [g_{\alpha}(\vec{x}, t) - g_{\alpha}^{eq}(\vec{x}, t)] \tag{2}$$

where  $\vec{x}' = \vec{x} + \vec{e}_\alpha \cdot \delta t$ ,  $\tau_f$  and  $\tau_g$  characterize the single relaxation times resulting from the BGK approximation for the collision operator, and the equilibrium density distribution functions are given as:

$$f_\alpha^{eq} = w_\alpha \rho \left[ 1 + 3 \frac{\vec{e}_\alpha \cdot \vec{u}}{c^2} + \frac{9}{2} \frac{(\vec{e}_\alpha \cdot \vec{u})^2}{c^4} - \frac{3}{2} \frac{\vec{u}^2}{c^4} \right] \tag{3}$$

$$g_\alpha^{eq} = w_\alpha \theta \left[ 1 + 3 \frac{\vec{e}_\alpha \cdot \vec{u}}{c^2} \right] \tag{4}$$

where  $w_0 = \frac{4}{9}$ ,  $w_\alpha = \frac{1}{9}$  for  $\alpha = 1, 2, 3, 4$ ,  $w_\alpha = \frac{1}{36}$  for  $\alpha = 5, 6, 7, 8$ ,  $\vec{u} = (u, v)$  and  $\vec{e}_\alpha$  denote the discrete velocities of the D2Q9 model are defined as:

$$\begin{cases} \vec{e}_\alpha = (0, 0) & \alpha = 0 \\ \vec{e}_\alpha = (\pm c, 0) & \alpha = 1, 2, 3, 4 \\ \vec{e}_\alpha = (\pm c, \pm c) & \alpha = 5, 6, 7, 8 \end{cases} \tag{5}$$

The macroscopic density, velocity and temperature are calculated by summing the distribution functions over the nine-velocity directions, as:

$$[\rho, \rho \vec{u}, \theta] = \sum_{\alpha=0-9} [f_\alpha, \vec{e}_\alpha f_\alpha, g_\alpha] \tag{6}$$

The continuity, momentum and energy equations can be recovered through the Chapman-Enskog expansion (He and Luo (1997)) under incompressible limit assumption ( $Ma = |\vec{u}|/c_s \ll 1$ ) and without forcing term, as:

$$\begin{cases} \nabla \cdot \vec{u} = 0 \\ \partial_t \vec{u} + \nabla \cdot (\vec{u} \vec{u}) = -(\nabla p)/\rho + \nu \nabla^2 \vec{u} \\ \partial_t \theta + \nabla \cdot (\vec{u} \theta) = \chi \nabla^2 \theta \end{cases} \tag{7}$$

where  $p = \rho c_s^2$  is the pressure from the equation of the state for the ideal gas,  $c_s = \frac{c}{\sqrt{3}}$  is the sound speed. The kinetic viscosity and the thermal diffusivity are linked to the relaxation times:

$$\tau_f = 3\nu + 0.5, \quad \tau_g = 3\chi + 0.5 \tag{8}$$

In simulating natural convection problem the additional forcing term is modeled under the Boussinesq approximation; which considers that all fluid properties are constant, except the fluid density given by  $\rho = \rho_0 (1 - \beta (T - T_r))$ , where  $\rho_0$  is a reference fluid density, then the external buoyant force  $\rho_0 \vec{G} = -\rho_0 \beta (T - T_r) \vec{g}$  appearing in momentum equation will be expressed as

$$F_\alpha = \frac{\vec{G} \cdot (\vec{e}_\alpha - \vec{u})}{c_s^2} f_\alpha^{eq} \tag{9}$$

Following these considerations  $|\vec{u}| \ll e_\alpha, f_\alpha^{eq} \approx w_\alpha \rho(x, t)$  and  $T_r = 0$ , the final form of the external body force is  $F_\alpha = -3w_\alpha \rho(\vec{x}, t) \beta T(\vec{x}, t) \vec{g} \cdot \vec{e}_\alpha$ .

For the boundary condition implementation, the no-slip boundary condition along the four walls is used using the bounce-back rule as:  $f_\alpha = f_\beta$ , where the asterisk " $\alpha$ " and " $\beta$ " denote opposite directions at the wall node. For the temperature field, the temperature distribution functions at the isothermal walls obey:  $g_\alpha = -g_\beta + (w_\alpha + w_\beta)T_{wall}$ . The adiabatic boundary condition is transferred to Dirichlet-type condition using the conventional second-order finite difference approximation as:  $g_{wall} = (4g_1 - g_2)/3$ .

### 2.3 Dimensionless parameters

Besides, in natural convection problems a characteristic velocity  $U = \sqrt{g\beta\Delta TH}$  is used as a reference scale to check the compressibility limit; and for the sake of comparison with previous findings, all predicted quantities are scaled using the reference quantities:  $L_0 = H, U_0 = \chi/H, t_0 = H^2/\chi, p_0 = \rho_0 U_0^2$  and  $\Delta T = T_h - T_c$  used for length, velocity, time, pressure and relative temperature respectively. The flow is characterized by the Prandtl number  $Pr = \nu/\chi$  set to 0.71, the Grashof number  $Gr = g\beta\Delta TH^3/\nu^2$  ranging from  $10^4$  to  $10^6$  and the average Nusselt number  $Nu_0$  along the source width calculated using a second order finite difference scheme as:

$$Nu_0 = \frac{1}{\varepsilon} \sum (3\theta_{i,0} - 4\theta_{i,1} + \theta_{i,2})/2 \tag{10}$$

The following convergence criteria is adopted in the present study,

$$\left| \frac{Nu_0(t) - Nu_0(t + 5000)}{Nu_0(t)} \right| \leq 10^{-4} \tag{11}$$

## 3 Results and discussion

### 3.1 Benchmarking the LB thermal model

To establish the credibility of the present lattice Boltzmann thermal model, a comparison test is made with former numerical finding using different computational approaches such as finite difference method (Aydin et al. (2000)), finite element method (Saha et al (2007)) and Lattice Boltzmann method coupled with finite difference technique (Che Sidik.N.A (2009)) for a centered heat source for  $\varepsilon=0.4$  and  $Gr=10^3$  or  $10^6$ .

Figure 3 illustrates a comparison of streamlines and isotherms plots for  $Gr=10^3$  and  $10^6$ , we can remark a good agreement between the two results for the thermal and dynamic structures. Figure 4 shows the Nusselt number variation under Grashof

number increase. It is well demonstrated through Figure 4, the excellent agreement between the three approaches.

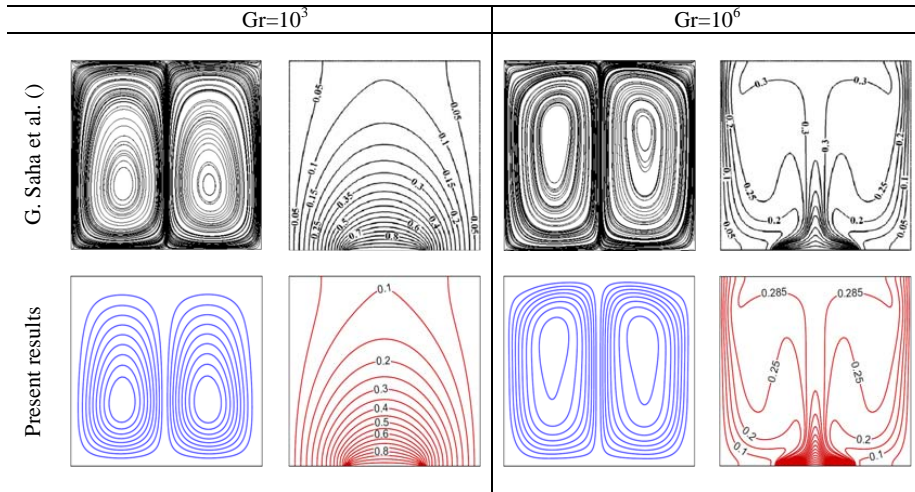


Figure 3: Comparison of the present predictions with reference results: streamlines (blue) and isotherms (red) for a centered hot source of length  $\epsilon=0.4$  at  $Gr=10^3$  and  $10^6$ .

We can state that this validation test allows us to use the present code in the following to investigate natural convection flow and heat transfer in square enclosure for the same range of Grashof number for different source lengths and positions.

In all performed numerical simulations, we'll take  $Pr = 0.71$ , which corresponds to air. First, we'll investigate the Grashof number effects ranging from  $10^4$  to  $10^6$  on the dynamic and thermal structures and heat transfer rate for the normalized length of the hot source  $\epsilon = 0.1$  centered at  $x_c=0.45$ . Second, the Grashof number is fixed to  $Gr=10^5$ , the source length is chosen  $\epsilon = 0.1$  and we investigate the effect of varying the source position for  $x_c=0.15, 0.25, 0.35$  and  $0.45$ . Finally, we investigate the effects of varying the hot source length (then  $\epsilon$  and  $x_c$  change conjointly for an asymmetrically heated enclosure), for  $Gr = 10^5$ . A uniform grid size of  $201 \times 201$  elements for  $Gr \leq 10^5$  and a grid size of  $301 \times 301$  for  $Gr = 10^6$  are used in the problem solution which we consider adequate to describe correctly the flow and heat transfer processes.

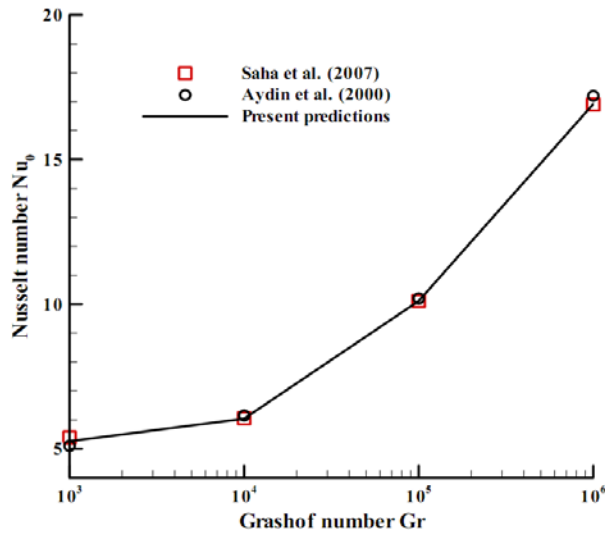


Figure 4: Comparison of the average Nusselt number versus Grashof number along hot wall for a centered hot source of length  $\varepsilon=0.2$  with previous findings

### 3.2 Grashof number effect

Figure 5 presents the effect of Grashof number ranging from  $10^4$  to  $10^6$ , for a source length  $\varepsilon=0.1$  and  $x_c=0.45$ , on the dynamic and thermal fields. First at all, one can remark the non-symmetric structures for streamlines and isotherms due to partially asymmetric heating. The deformation of isotherms increases with increasing the Grashof number and the thermal boundary layers are more stratified owing to intensification of flow circulation. This indicates that the main heat transfer mechanism is enhanced by convection currents. The effect of convection currents intensity can be seen from the streamlines; for different Gr, the flow pattern is characterized by two rolls with clockwise and anticlockwise rotations inside the enclosure. The flow ascends toward the upper adiabatic wall, owing to the important attractive effect by each cold wall, the flow turns horizontally then it moves downwards along vertical walls. After, the flow moves horizontally to supply again the hot source. For  $Gr=10^4$ , we note a slight tilting of the flow toward vertical right wall. In addition, the flow circulation inside the enclosure is weak due to dominance of conduction mode of heat transfer than the convection. With increasing Gr to  $10^6$ , the recirculation becomes strong, the cores of rolls move upward and the streamlines are more deviated toward cold left wall. This indicates the predominance of the buoyancy force than viscous forces.

Figure 6 shows the surface-averaged Nusselt number along the hot source,  $Nu_0$ , as a function of Grashof number for source length  $\varepsilon = 0.1$  with fixed position  $x_c = 0.45$ . For low Grashof number  $10^3 \leq Gr \leq 10^4$ , we note a slight growth rate of the average Nusselt number owing to low thermal gradients and predominance of conduction regime. With increasing  $Gr$  to  $10^6$ , Nusselt Number increases quickly to reach its higher value.

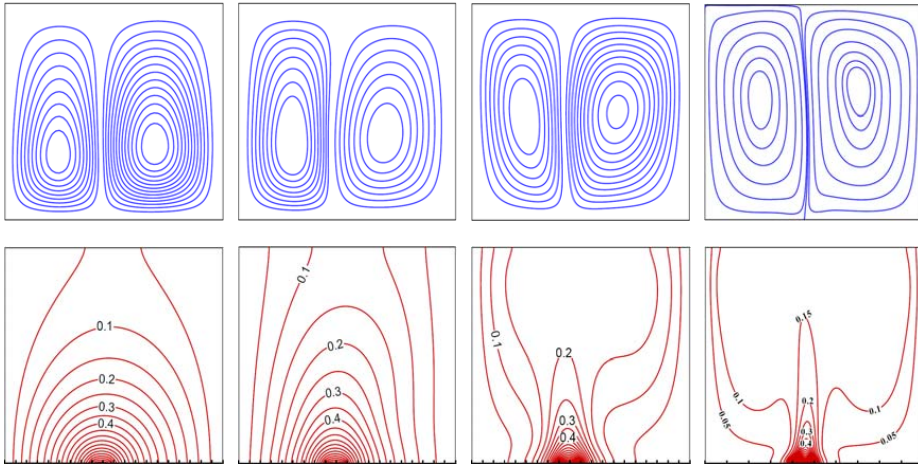


Figure 5: Effect of Grashof number on streamlines (blue) and isotherms (red) distributions for  $10^4 \leq Gr \leq 10^6$ ,  $\varepsilon = 0.1$  and  $x_c = 0.45$

### 3.3 Hot source position effect

Focus is made in this section on the the source position effect on the flow behavior inside the square enclosure for a Grashof number  $Gr = 10^5$  and source length  $\varepsilon = 0.1$ . Four source-centre positions are treated, say:  $x_c = 0.15, 0.25, .35$  and  $0.45$ . The results for temperature and streamlines distributions are depicted in Fig. 7.

For low hot source position ( $x_c = 0.15$ ), the wall jet formed due to the right intake (supply) blocks the thermal plume against the left cold wall leading to formation of a small rotating cell of the left of the hot source. The plume is, after that, deformed to the right at mid-height and goes up vertically to the cavity ceiling, leading to a second vortex cell greater than the first indicated. One can remark, also, that the plume is not too developed and the isotherms are tight around the sources. The averaged Nusselt number is close to 14.95. Increasing the source position to 0.25, the plume is more tilted counter the left wall and more developed vertically compared to the case  $x_c = 0.15$ , and the two secondary cells are more enlarged. The Nusselt

number decreases slightly (-1.34%) to be 14.75. For  $x_c=0.35$ , the secondary small cells begin the merge and are surrounded by a one cell. This indicates a threshold of cells merging slightly little than 0.35. The plume is seen more outcropped than last two cases. The heat transfer rate decreases more to 14.67, than -0.6% compared to 14.75. For  $x_c=0.45$ , the secondary cells are completely merged and two strong cells occupy the hole of the cavity. The asymmetrically heating is clearly put on view by the two big counter rotating cells with two different sizes. A thermal stratification is formed near cold walls at the upper mid-height. The Nusselt number is close to 14.21. The global heat transfer decrease compared to the case  $x_c=0.15$  is, then, about 5%.

The little variation in the heat transfer amount quantified by the average Nusselt number is well explained by plotting the local Nusselt number along the hot source, the results are depicted in Fig. 8. As one can remark, for  $x_c=0.15$ , the local Nusselt number at left source side is the highest from the four cases, this certainly due to its existence in the vicinity of the cold wall where the small vortex turns in the sense of entraining cold air toward the hot source than enhancing the cooling. The left local Nusselt number evolves in a parabolic behavior with increasing the hot source position with a minima between  $x=0.25$  and  $0.3$  corresponding to the secondary cells merging, as mentioned here-before. Besides, the local right Nusselt number enhanced by right-lateral aspiration of cold air (supply) evolves contrarily, in such a way the two values are equalized for a centered hot source.

### **3.4 Source length effect**

Figure 9 shows the streamlines and isotherms plots versus source length  $\varepsilon$  for  $Gr = 10^5$ . The cavity is partially heated from below from  $x=0.4$  to  $0.5$  ( $\varepsilon =0.1$ ), from  $x=0.3$  to  $0.5$  ( $\varepsilon =0.2$ ), from  $x=0.2$  to  $0.5$  ( $\varepsilon =0.3$ ) and from  $x=0.1$  to  $0.5$  ( $\varepsilon =0.4$ ). For  $\varepsilon =0.2$ , the thermal behavior is nearly the same as for  $\varepsilon =0.1$ ; however for the dynamic field the left rotating cell size is reduced and is pushed at its center by the right cell. Increasing the source length to  $\varepsilon =0.3$ , the thermal contours are more pushed toward the left cold wall, with a deflection of isotherms around  $y=0.75$  which corresponds to the existence of the secondary higher cell formed at the top-left corner of the cavity. The dynamic field is then a three rotating cells structure. Thermal stratification is formed near the right cold wall and the thermal gradients in the vicinity of the hot source are reduced; this can be deduced from the isotherm levels which show that the plume is more developed toward the upper wall. Increasing more the source length to  $\varepsilon =0.4$ , one can remark that the principal roll pushes the link point of the two minor roll to move-down, then the lower cell size is reduced.

The effect of increasing the length source, then the buoyancy intensity, is more

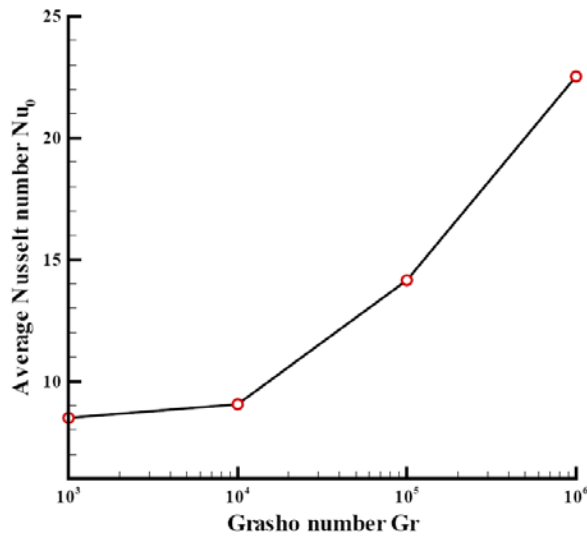


Figure 6: Surface-averaged Nusselt number along the hot source vs Grashof number  $\varepsilon = 0.1$  and  $x_c = 0.45$ .

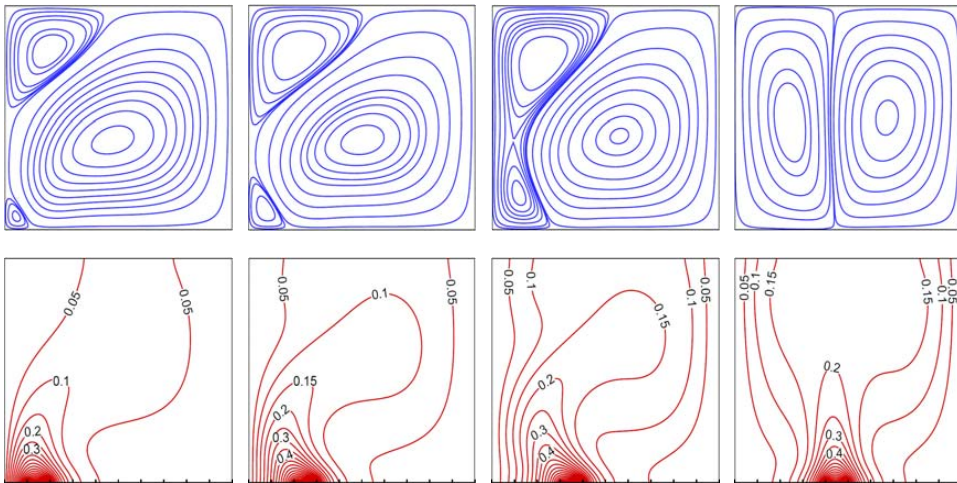


Figure 7: Streamlines (blue) and isotherms (red) plots versus source position  $x_c$  for  $\varepsilon = 0.1$  and  $Gr = 10^5$ .

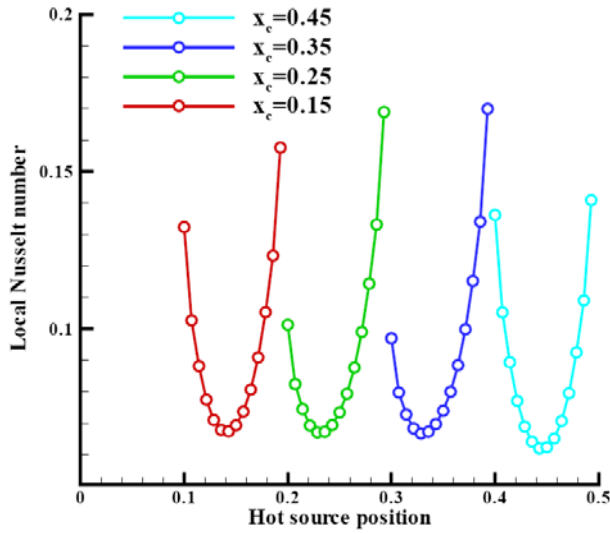


Figure 8: Local Nusselt number variation along hot source for  $\epsilon = 0.1$  and  $Gr=10^5$ .

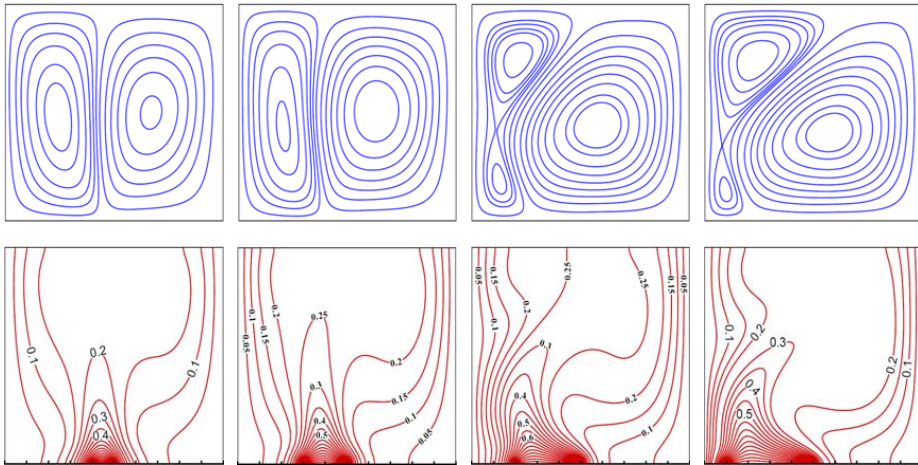


Figure 9: Streamlines (blue) and isotherms (red) plots versus source length  $\epsilon$  for  $Gr=10^5$ .

apparent through the isotherm and Streamtraces profiles. This conclusion is verified through the heat transfer rate computed along the hot source: the Nusselt number is close to 14.21, 10.96, 9.38 and 8.53 for respectively  $\varepsilon = 0.1, 0.2, 0.3$  and  $0.4$ . Heat transfer is then enhanced by increasing the source length when regarding to Nusselt number non-averaged by hot source area.

#### 4 Conclusion

In more of two decades the lattice Boltzmann method plays important role in computational fluid dynamics by the computational facilities provided by simple coding in many coordinate systems and by the high level of accuracy and preserving the computational cost. In the present study a double population thermal lattice Boltzmann model D2Q9-D2Q9 is developed to investigate the effects of partially heating a cavity from below. Three main parameters effects are studied, namely the effect of increasing the Grashof number, varying the *hot source position* and the *source length* for the case of *asymmetrically heating*.

It has been concluded that increasing the Grashof number results in enhancing the natural convection inside the enclosure and then increasing the heat transfer rate; besides, increasing the hot source length affects greatly the dynamic and thermal structures as well as the heat transfer rate quantified by the integral Nusselt number along the hot source. However, for the hot source position the heat transfer is not greatly affected even there is a considerable change in the dynamic and thermal behaviours.

This study presents some basic understanding of natural convection flows and heat transfer characteristics in partially and asymmetrically heated enclosures from below in laminar regime. Our future works will focus on the study of turbulent characteristics of thermal plumes evolving in free / confined media since this area is encountered in numerous applied cases of thermal engineering [see Naffouti et al. (2009); Naffouti, Zinoubi, and Ben Maad (2010)].

**Acknowledgement:** The second author gratefully acknowledges Prof. Z. Guo (Huazhong University of Science and Technology, Wuhan, China) for fruitful discussions about basics of the lattice Boltzmann method and thanks particularly the University of Limoges for the computational facilities provided by CALI calculation center.

#### References

**Alama, P.; Kumar, A.; Kapoor, S.; Ansari, S.R.** (2012): Numerical investigation of natural convection in a rectangular enclosure due to partial heating and cooling at

- vertical walls. *Commun. Nonlinear Sci. Numer. Simulat.*, vol. 17, pp. 2403-2414.
- Aydin, O.; Yang, J.** (2000): Natural convection in enclosure with localized heating from below and symmetrically cooling from sides. *Int. J. of Numerical Methods of Heat and Fluid Flow*, vol. 10, no. 5, pp. 518-529.
- Calgagni, B.; Marsili, F.; Paroncini, M.** (2005): Natural convection heat transfer in square enclosures heated from below. *Appl. Thermal Engineering*, vol. 25, no. 16, pp. 2522-2531.
- Chatterjee, D.** (2010): Lattice Boltzmann simulation of incompressible transport phenomena in macroscopic solidification processes. *Num. Heat Transfer, Part B: Fundamentals*, vol. 58, no. 1, pp. 55-72.
- Che Sidik, N.A.** (2009): Prediction of natural convection in a square cavity with partially heated from below and symmetrical cooling from sides by the finite difference Lattice Boltzmann Method. *European Journal of Scientific Research*, vol. 35, no. 3, pp.347-354.
- Che Sidik, N.A., Izual, N.I.N.** (2012): Numerical Investigation of Fluid and Thermal Flow in a Differentially Heated Side Enclosure Walls at Various Inclination Angles. *CMES: Computer Modeling in Engineering & Sciences*, vol. 84, no. 6, pp. 559-574.
- Chu, T.Y.; Hichox, C.E.** (1990): Thermal convection with large viscosity variation in an enclosure with localized heating. *J. of Heat Transfer*, vol.112, no. 2, pp. 388-395.
- Corcione, M.** (2003): Effects of the thermal boundary conditions at the sidewalls upon natural convection in rectangular enclosures heated from below and cooled from above. *Int. J. of Thermal Sciences*, vol. 42, no. 2, pp.199-208.
- Djebali, R.; El Ganaoui, M.** (2011): Assessment and Computational Improvement of Thermal Lattice Boltzmann Models Based Benchmark Computations. *CMES: Computer Modeling in Engineering & Sciences*, vol. 71, n. 3, pp. 179-202.
- Djebali, R.; El Ganaoui, M.; Pateyron, B.** (2012): A Lattice Boltzmann Based Investigation of Powder In-flight Characteristics during APS Process, Part I: Modelling and Validation. *Progress in Computational Fluid Dynamics: an int. Journal*, vol. 12, n. 4, pp. 270-278.
- Djebali, R.; El Ganaoui, M.; Naffouti, T.** (2012): A 2D Lattice Boltzmann Full Analysis of MHD Convective Heat Transfer in Saturated Porous Square Enclosure. *CMES: Computer Modeling in Engineering & Sciences*, vol. 84, n. 6, pp.499-527.
- Djebali, R.; Pateyron, B.; El Ganaoui, M.** (2011): A lattice Boltzmann-Based Study of Plasma Sprayed Particles Behaviours. *CMC: Computers, Materials & Continua*, vol. 25, n. 2, pp. 159-176.

**Djebali, R.; Sammouda, H.; El Ganaoui, M.** (2010): Some Advances in Applications of Lattice Boltzmann Method for Complex Thermal Flows. *Adv. Appl. Math. Mech.*, vol. 2, n. 5, pp. 587-608.

**Ganzorolli, M.M.; Milanez, L.F.** (1995): Natural convection in rectangular enclosures heated from below and symmetrically cooled from the sides. *Int. J. of Heat and Mass Transfer*, vol. 38, no. 6, pp. 1063-1073.

**Guo, Z.; Zhao, T. S.** (2005): A Lattice Boltzmann model for convection heat transfer in porous media. *Num. Heat Transfer, Part B: Fundamentals*, vol. 47, no. 2, pp. 157-177.

**Hasnaoui, M.; Bilgen, E.; Vasseur, P.** (1992): Natural convection heat transfer in rectangular cavities partially heated from below. *J. of Thermophysics Heat Transfer*, vol.6, no. 2, pp. 255-264.

**He, X.; Luo, L.S.** (1997): Lattice Boltzmann Model for the incompressible Navier-Stokes equation. *Journal of statistical Physics*, vol. 88, no. 3/4, pp. 927-944.

**Lakhal, E.K.; Hasnaoui, M.; Vasseur, P.; Bilgen, E.** (1995): Natural convection in a square enclosure heated periodically from part of the bottom wall. *Numer. Heat Transfer*, vol. 27, no. 3, pp. 319-333.

**Lou, Q.; Guo, Z.; Zheng, C.** (2011): Some Fundamental Properties of Lattice Boltzmann Equation for Two Phase Flows. *CMES: Computer Modeling in Engineering & Sciences*, vol. 76, no. 3, pp. 175-188.

**Massimo, P.; Francesco, C.; Maria, M. D. P.** (2006): Study and analysis of the influence of a small heating source position on the natural convective heat transfer in a square cavity. *Proceedings of the 4th WSEAS Int. Conf. on Heat Transfer, Thermal Engineering and Environment*, pp. 305-310.

**Naffouti, T.; Hammami, M.; Rebay, M.; Ben Maad, R.** (2009): Experimental study of a thermal plume evolving in a confined environment: Application to fires problems. *Journal of Applied Fluid Mechanics*, vol. 2, no. 1, pp. 29-38.

**Naffouti, T.; Zinoubi, J.; Ben Maad, R.** (2010): Experimental characterization of a free thermal plume and in interaction with its material environment. *Journal of Applied thermal engineering*, vol. 33, no. 13, pp. 1632-1643.

**Paroncini, M.; Corvaro, F.** (2009): Natural convection in a square enclosure with a hot source. *Int. J. of Therm.*, vol. 48, no. 9, pp. 1683-1695.

**Ramos, R.A.V.; Milanez, L.F.** (1998): Numerical and experimental analysis of natural convection in a cavity heated from below. *Proc. 11th IHTC, Kyongju, Korea*, vol. 3, no. 8, pp. 531-535.

**Saha, G.; Saha, S.; Quamrul Islam, M.; Razzaq Akhanda, M.A.** (2007): Natural convection in enclosure with discrete isothermal heating from below. *Journal*

*of Naval Architecture and Marine Engineering*, vol. 4, no. 1, pp. 1-13.

**Sarris, I.E.; Lekakis, I.; Vlachos, N.S.** (2004): Natural convection in rectangular tanks heated locally from bellow. *Int. J. of Heat and Mass Transfer*, vol. 47, no. 14/16, pp. 3549-3563.

**Sharif, AMR. M.; Mohammad T.R.** (2005): Natural convection in cavities with constant flux heating at the bottom wall and isothermal cooling from the sidewalls. *Int. J of Thermal Sciences*, vol. 44, no. 9, pp. 865-878.

**Turgoklu, H.; Yucel, N.** (1995): Effect of heater and cooler locations on natural convection in square cavities. *Numer. Heat Transfer*, vol. 27, no. 3, pp. 351-358.

